

Title	First Measurement of the Neutron beta Asymmetry with Ultracold Neutrons
Author(s)	Pattie, RW; Anaya, J; Back, HO; Boissevain, JG; Bowles, TJ; Broussard, LJ; Carr, R; Clark, DJ; Currie, S; Du, S; Filippone, BW; Geltenbort, P; Garcia, A; Hawari, A; Hickerson, KP; Hill, R; Hino, M; Hoedl, SA; Hogan, GE; Holley, AT; Ito, TM; Kawai, T; Kirch, K; Kitagaki, S; Lamoreaux, SK; Liu, CY; Liu, J; Makela, M; Mammei, RR; Martin, JW; Melconian, D; Meier, N; Mendenhall, MP; Morris, CL; Mortensen, R; Pichlmaier, A; Pitt, ML; Plaster, B; Ramsey, JC; Rios, R; Sabourov, K; Sallaska, AL; Saunders, A; Schmid, R; Seestrom, S; Servicky, C; Sjue, SKL; Smith, D; Sondheim, WE; Tatar, E; Teasdale, W; Terai, C; Tipton, B; Utsuro, M; Vogelaar, RB; Wehring, BW; Xu, YP; Young, AR; Yuan, J
Citation	PHYSICAL REVIEW LETTERS (2009), 102(1)
Issue Date	2009-01-09
URL	<a href="http://hdl.handle.net/2433/84642">http://hdl.handle.net/2433/84642</a>
Right	© 2009 The American Physical Society
Type	Journal Article
Textversion	publisher

## First Measurement of the Neutron $\beta$ Asymmetry with Ultracold Neutrons

R. W. Pattie, Jr.,<sup>1,2</sup> J. Anaya,<sup>3</sup> H. O. Back,<sup>1,2</sup> J. G. Boissevain,<sup>3</sup> T. J. Bowles,<sup>3</sup> L. J. Broussard,<sup>2,4</sup> R. Carr,<sup>5</sup> D. J. Clark,<sup>3</sup> S. Currie,<sup>3</sup> S. Du,<sup>1</sup> B. W. Filippone,<sup>5</sup> P. Geltenbort,<sup>6</sup> A. García,<sup>7</sup> A. Hawari,<sup>8</sup> K. P. Hickerson,<sup>5</sup> R. Hill,<sup>3</sup> M. Hino,<sup>9</sup> S. A. Hoedl,<sup>7,10</sup> G. E. Hogan,<sup>3</sup> A. T. Holley,<sup>1</sup> T. M. Ito,<sup>3,5</sup> T. Kawai,<sup>9</sup> K. Kirch,<sup>3</sup> S. Kitagaki,<sup>11</sup> S. K. Lamoreaux,<sup>3</sup> C.-Y. Liu,<sup>10</sup> J. Liu,<sup>5</sup> M. Makela,<sup>3,12</sup> R. R. Mammei,<sup>12</sup> J. W. Martin,<sup>5,13</sup> D. Melconian,<sup>7,14</sup> N. Meier,<sup>1</sup> M. P. Mendenhall,<sup>5</sup> C. L. Morris,<sup>3</sup> R. Mortensen,<sup>3</sup> A. Pichlmaier,<sup>3</sup> M. L. Pitt,<sup>12</sup> B. Plaster,<sup>5,15</sup> J. C. Ramsey,<sup>3</sup> R. Rios,<sup>3,16</sup> K. Sabourov,<sup>1</sup> A. L. Sallaska,<sup>7</sup> A. Saunders,<sup>3</sup> R. Schmid,<sup>5</sup> S. Seestrom,<sup>3</sup> C. Servicky,<sup>1</sup> S. K. L. Sjue,<sup>7</sup> D. Smith,<sup>1</sup> W. E. Sondheim,<sup>3</sup> E. Tatar,<sup>16</sup> W. Teasdale,<sup>3</sup> C. Terai,<sup>1</sup> B. Tipton,<sup>5</sup> M. Utsuro,<sup>9</sup> R. B. Vogelaar,<sup>12</sup> B. W. Wehring,<sup>8</sup> Y. P. Xu,<sup>1</sup> A. R. Young,<sup>1,2</sup> and J. Yuan<sup>5</sup>

(UCNA Collaboration)

<sup>1</sup>*Department of Physics, North Carolina State University, Raleigh, North Carolina 27695, USA*

<sup>2</sup>*Triangle Universities Nuclear Laboratory, Durham, North Carolina 27708, USA*

<sup>3</sup>*Los Alamos National Laboratory, Los Alamos, New Mexico 87545, USA*

<sup>4</sup>*Department of Physics, Duke University, Durham, North Carolina 27708, USA*

<sup>5</sup>*W. K. Kellogg Radiation Laboratory, California Institute of Technology, Pasadena, California 91125, USA*

<sup>6</sup>*Institut Laue-Langevin, 38042 Grenoble Cedex 9, France*

<sup>7</sup>*Physics Department, University of Washington, Seattle, Washington 98195, USA*

<sup>8</sup>*Department of Nuclear Engineering, North Carolina State University, Raleigh, North Carolina 27695, USA*

<sup>9</sup>*Research Reactor Institute, Kyoto University, Kumatori, Osaka, 590-0401, Japan*

<sup>10</sup>*Physics Department, Princeton University, Princeton, New Jersey 08544, USA*

<sup>11</sup>*Tohoku University, Sendai 980-8578, Japan*

<sup>12</sup>*Department of Physics, Virginia Tech, Blacksburg, Virginia 24061, USA*

<sup>13</sup>*Department of Physics, University of Winnipeg, Winnipeg, MB R3B 2E9, Canada*

<sup>14</sup>*Cyclotron Institute, Texas A&M University, College Station, Texas 77843, USA*

<sup>15</sup>*Department of Physics and Astronomy, University of Kentucky, Lexington, Kentucky 40506, USA*

<sup>16</sup>*Department of Physics, Idaho State University, Pocatello, Idaho 83209, USA*

(Received 17 September 2008; published 5 January 2009)

We report the first measurement of an angular correlation parameter in neutron  $\beta$  decay using polarized ultracold neutrons (UCN). We utilize UCN with energies below about 200 neV, which we guide and store for  $\sim 30$  s in a Cu decay volume. The interaction of the neutron magnetic dipole moment with a static 7 T field external to the decay volume provides a 420 neV potential energy barrier to the spin state parallel to the field, polarizing the UCN before they pass through an adiabatic fast passage spin flipper and enter a decay volume, situated within a 1 T field in a  $2 \times 2\pi$  solenoidal spectrometer. We determine a value for the  $\beta$ -asymmetry parameter  $A_0 = -0.1138 \pm 0.0046 \pm 0.0021$ .

DOI: 10.1103/PhysRevLett.102.012301

PACS numbers: 14.20.Dh, 12.15.Ff, 12.15.Hh, 23.40.Bw

Measurements of neutron  $\beta$  decay observables provide fundamental information on the parameters characterizing the weak interaction of the nucleon. Results from such measurements can be used to extract a value for the CKM quark-mixing matrix element  $V_{ud}$  and impact predictions for the solar neutrino flux, big bang nucleosynthesis, the spin content of the nucleon, and tests of the Goldberger-Treiman relation [1]. High-precision results also place constraints on various extensions to the standard model, such as supersymmetry [2] and left-right symmetries [3]. Angular correlation measurements in neutron  $\beta$  decay have been performed with thermal and cold neutron beams [4], including all previously reported measurements of the  $\beta$  asymmetry [5–9]. The use of UCN for these measurements provides a different and powerful approach to controlling key sources of systematic effects in mea-

surements of polarized neutron  $\beta$  decay: the preparation of highly polarized neutrons and the backgrounds intrinsic to the neutron  $\beta$  decay sample.

The angular distribution of emitted electrons is

$$W(E_e, \theta) = F(E_e)(1 + A\langle P\rangle\beta \cos\theta), \quad (1)$$

where  $E_e$  and  $\beta$  are the electron energy and velocity relative to  $c$ ,  $F(E_e)$  is the allowed shape of the electron energy spectrum,  $\langle P\rangle$  is the neutron polarization, and  $\theta$  is the angle between the neutron spin and the electron momentum. The  $\beta$  asymmetry is given by  $A = A_0(1 + a_0 + a_{-1}/E_e + a_{+1}E_e)(1 + \delta)$ , where  $A_0 = -2\lambda(\lambda + 1)/(1 + 3\lambda^2)$  [10]. The recoil order terms  $a_0$ ,  $a_{-1}$ ,  $a_{+1}$  and the radiative correction  $\delta$  are specified in the standard model and dominated by three coupling constants:  $g_v$  and  $g_a$  (vector and axial vector, with  $\lambda \equiv g_a/g_v$ ), and  $g_{wm}$

(weak magnetism). Three additional form factors are expected to be negligible at the level of precision of this work. Very precise estimates for  $g_v$  and  $g_{wm}$  are available in the standard model, but precise theoretical predictions for  $g_a$  are not available. Other than  $g_a$ , limiting theoretical uncertainties are below the 0.1% level, and stem from hadronic loop contributions to radiative corrections [11].

UCN are defined as neutrons with energies low enough ( $\leq 340$  neV) that they undergo total external reflection from an effective potential barrier  $E_{\text{Fermi}}$  at some material surfaces [12] and can thus be stored in material bottles. We produced UCN in a solid deuterium ( $\text{SD}_2$ ) source [13] coupled to a tungsten spallation target in the 800 MeV proton beam at the Los Alamos Neutron Science Center (LANSCE). Protons were delivered in 28  $\mu\text{C}$  pulses, once every 17 s, with the spallation neutrons moderated in cold ( $\sim 20$  K) polyethylene surrounding the source. UCN were created via downscattering of the resulting cold neutron flux in 5 K  $\text{SD}_2$ . After each proton pulse, the emerging UCN passed through a valve located above the  $\text{SD}_2$ . This valve was then closed, loading a storage volume (20 l vertical volume and 40 l of guides) above the  $\text{SD}_2$  with an estimated density of 10 UCN  $\text{cm}^{-3}$  at the exit of the spallation source shielding. The vertical storage volume was coupled by about 5 m of electropolished stainless steel guides (with two 45° bends to limit backgrounds) to a gate valve just beyond the shielding, and then ultimately to a switcher which allowed the guides comprising the  $\beta$ -asymmetry experiment (see Fig. 1) to be connected either to the UCN source or a  $^3\text{He}$  UCN detector for depolarization measurements, described below.

One of the primary advantages of the low UCN energy is the ability to highly polarize a UCN population via the interaction of the neutron magnetic dipole moment

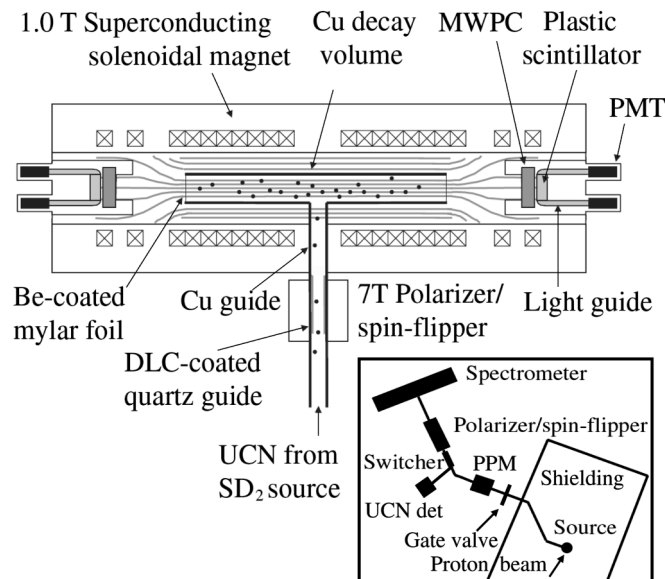


FIG. 1. Schematic (not to scale) of the  $\beta$ -asymmetry experiment. Inset depicts the layout of the UCN source and transport guides.

with a static magnetic field ( $\vec{\mu}_n \cdot \vec{B}$ ), which amounts to  $\pm 60$  neV  $\text{T}^{-1}$  for neutron spins aligned (+) or antialigned (−) with the field. The UCN were polarized via this effect, using a longitudinal 6 T field in a prepolarizer magnet (PPM) and a 7 T field in the primary polarizer and spin-flipper magnet. The polarization of the subsequent population was maintained by polarization-preserving electropolished Cu ( $E_{\text{Fermi}} \approx 168$  neV) guides and a 100-cm long diamondlike carbon (DLC) coated quartz section ( $E_{\text{Fermi}} > 200$  neV) passing through the center of a resonant “bird-cage” rf cavity used for adiabatic fast passage (AFP) spin flipping of the UCN. Overlapping fringe fields served as the holding field between the polarizer and spectrometer magnets.

Prior to the  $\beta$ -asymmetry run, a measurement of the AFP spin-flipper efficiency was made by placing the PPM magnet after the polarizer and spin-flipper magnet, creating a crossed polarizer analyzer with the PPM utilized as the analyzer. The transmission through the system was measured to be 0.40(5)%, placing a lower limit of 99.1% on the initial UCN polarization and a lower limit of 99.6% on the spin-flipper efficiency.

In order to measure the depolarization on a run-by-run basis during the  $\beta$ -asymmetry measurement, the measurement cycle consisted of a background run (with proton beam on, but gate valve closed, resulting in no UCN in the spectrometer,  $\sim 720$  s in duration) followed by the  $\beta$ -asymmetry measurement for some spin state ( $\sim 3600$  s), and then a measurement of the depolarized population ( $\sim 240$  s). The depolarization measurement consisted of first closing the gate valve while simultaneously connecting the guides at the upstream side of the experiment to the  $^3\text{He}$  UCN detector using the switcher. This cleaning phase, lasting 150 s, allowed the number of correctly polarized UCN downstream of the 7 T polarizing field to be measured. Next, the depolarized population present in the experiment was unloaded and counted by changing the state of the spin flipper. Counting during this unloading cycle was carried out for 100 s. The depolarized contamination at the end of each individual run was consistent with zero. By combining all available runs, correcting for depolarized UCN detection efficiency, and attributing the crossed polarizer analyzer result entirely to unpolarized UCN, we were able to place an upper limit ( $1\sigma$ ) of 0.65% on the depolarized fraction present during any individual run. We expect that better characterization of our system combined with significant improvements in background and statistics during depolarized UCN counting should result in a limit below 0.2% in the future.

After transport to the spectrometer, the UCN were confined to a 300-cm long, 12-cm diameter Cu decay trap tube with end-cap foils consisting of 2.5- $\mu\text{m}$  thick mylar foils coated with 300 nm of Be. Storage times of  $\sim 30$  s were achieved, limited by gaps in the guide and decay trap geometry, resulting in a UCN density of about 0.2  $\text{cm}^{-3}$ . A plastic collimator with an inner diameter of 11.7 cm,

which also functioned as the end-cap foil mount, suppressed contamination from electrons scattering from the Cu decay trap or resulting from neutron capture on the Cu walls. The spectrometer's 1 T solenoidal field was oriented along the decay trap axis and provided for  $2 \times 2\pi$  collection of the  $\beta$  decay electrons, which spiraled along the field lines toward one of two identical electron detector packages [14]. A field-expansion region from 1 T in the decay volume to 0.6 T in the electron detector region suppressed electron backscattering events [15].

The two electron detector packages [15,16] each consisted of a low-pressure (132 mbar) multiwire proportional chamber (MWPC) backed by a 3.5-mm thick, 15-cm diameter plastic scintillator, and were spaced 4.4 m apart. The MWPCs permitted reconstruction (with 2 mm resolution) of the events' transverse coordinates, ensuring "edge effects" associated with electron scattering from the walls of our decay trap or collimator edges were negligible. The MWPCs were separated from the spectrometer vacuum and the scintillator volumes by identical 25- $\mu$ m thick mylar entrance and exit windows.

The scintillator, with an energy resolution of 5.6% at 1 MeV, generated the trigger and provided for the energy measurement. Energy calibrations were performed *in situ* every 6–8 h, using a  $^{113}\text{Sn}$  source of conversion electrons which could be inserted and retracted from the spectrometer's fiducial volume. Gain variations between calibrations were monitored and corrected for by comparing the response of the scintillator and an external photomultiplier tube (PMT) to a pulsed LED source. The response of the external PMT to the LED was normalized to the spectrum of gamma rays from a  $^{60}\text{Co}$  source in a NaI crystal coupled to this PMT.

The linearity of the detector response was studied with a limited selection of commercially available conversion-electron sources ( $^{113}\text{Sn}$  or  $^{207}\text{Bi}$  between 4  $\mu$ m thick plastic foils), effectively calibrating the detectors. Analysis of the implementation of our calibration via Monte Carlo calculations suggests a (conservative) 1.5% uncertainty in the value for  $A_0$  due to possible errors in our electron energy reconstruction.

Background rates were reduced from roughly  $40 \text{ s}^{-1}$  to  $1 \text{ s}^{-1}$  by requiring a coincidence between the same-side MWPC and scintillator. The spectrometer was surrounded by a cosmic-ray muon veto system consisting of proportional gas tubes and a plastic scintillator. Proton beam-related backgrounds were suppressed with timing cuts. After all cuts, the integrated background rate over the fiducial volume up to the endpoint was about  $0.2 \text{ s}^{-1}$ . A significant potential advantage of UCN over cold neutron beams for angular correlation measurements stems from the relatively small number of neutrons present in the decay geometry and guides. Because the absolute efficiency for detection of neutron-generated gamma-ray backgrounds by the MWPC-scintillator coincident system is extremely small compared to the nearly 100% electron-detection efficiency, UCN-generated backgrounds were negligible.

Misidentification of backscattering events is one of the largest contributions to the total fractional systematic correction to the value for  $A_0$  reported here (see Table I). Electrons triggering both scintillators within a 100 ns acceptance window comprised 2.5(3)% of all events, with the initial direction of incidence determined by the scintillators' relative trigger times. The bias to the asymmetry from events with transit times greater than 100 ns is small,  $<10^{-5}$ . Another class of backscattering events, comprising 1.4(2)% of the event fraction, were those events which triggered only one of the scintillators, but deposited energy in both MWPCs. Comparison of the energy deposition in the MWPCs determines the initial direction of incidence for these events, with the efficiency for this identification calculated in Monte Carlo to be  $\sim 80\%$ . Finally, events which backscattered from either the decay trap end-cap foils or the MWPC entrance windows could not be identified in data analysis, and are termed "missed" backscattering events. Corrections for these missed backscattering events were separately performed using the GEANT4 [17] and PENELOPE [18] simulation packages, and found to be 1.1(4)%. Previous studies of these Monte Carlo backscattering calculations suggest a 30% uncertainty in the missed backscattering correction [19].

Linear parametrizations of energy loss in the decay trap end-cap foils and the MWPC entrance or exit windows and interior were employed to reconstruct, on an event-by-event basis for each event type, the  $\beta$  decay energy from the measured energy deposition in the scintillator(s). The resulting energy spectrum, compared to background, is shown in Fig. 2. Disagreement between the shape of the reconstructed energy spectrum and that expected from simulation is  $<3\%$  over the chosen analysis region of 200–600 keV. The lower limit of 200 keV was constrained by energy loss for backscattering events triggering both scintillators. The upper limit of 600 keV was an optimization of the signal-to-noise ratio, seen in Fig. 2 to be 21:1 from 200–600 keV (over  $0.17 \text{ s}^{-1}$  of background), and also constrained by considerations of other systematics over the range 600–800 keV. Note that the background-subtracted rate above the  $\beta$  decay endpoint was consistent with zero.

Because of the angle dependence of the energy loss, the average value of  $\cos\theta$  deviates from 1/2 and varies as a

TABLE I. Fractional systematic corrections to  $A_0$ .

Systematic	Correction	Uncertainty
Polarization	-	0.013
UCN-Induced Backgrounds	-	0.002
Electron Detector Effects		
Response/Linearity	-	0.015
Gain Drifts	-	0.002
Electron Trajectories		
Angle Effects	-0.016	0.005
Backscattering	0.011	0.004
Total	$-5 \times 10^{-3}$	0.021

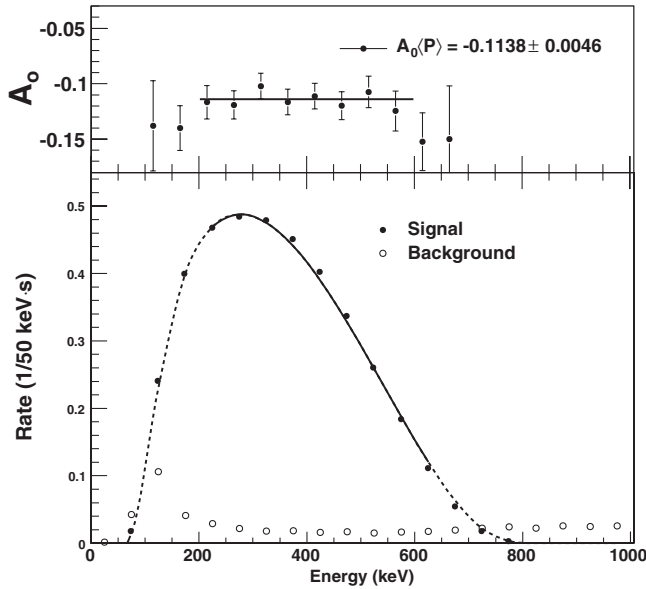


FIG. 2. Top panel: Values for  $A_0$  extracted from the best fit, varying the parameter  $\lambda$ , plotted as a function of the reconstructed  $\beta$  decay energy (i.e., after accounting for energy loss; see text for details). The value of the radiative corrections,  $\delta$ , is below 0.1% [20] and therefore negligible for this study. Bottom panel: Reconstructed  $\beta$  decay energy spectrum, summed over detectors, compared with the expectation from Monte Carlo calculations (dashed line). Solid line indicates analysis region.

function of energy. The correction to the asymmetry for such “angle effects” was calculated with the Monte Carlo simulation to be  $-1.6(5)\%$ . Effects due to differences in loading efficiencies for the two spin states and detector efficiencies cancel in a super ratio of rates,  $S(E_e) = r(E_e)_1 r(E_e)_2 / r(E_e)_1 r(E_e)_2$ , where  $r(E_e)_{1(2)}^{(1)}$  was the rate measured in detector 1(2) when the spin-flipper was on(off). The experimental asymmetry is then  $A(E_e) = (1 - \sqrt{S(E_e)}) / (1 + \sqrt{S(E_e)})$ . After correcting for backscattering and angle effects,  $A_0$  was extracted from a one-parameter fit. With these corrections we find  $A_0 = -0.1138(0.0046)_{\text{stat}}(0.0021)_{\text{syst}}$ . Results for  $A_0$  from independent analyses utilizing PENELOPE or GEANT4 for calculation of the corrections for energy loss and backscattering agreed to 0.26%.

In summary, we have demonstrated the first-ever measurement of a neutron  $\beta$  decay angular correlation parameter with UCN. Reduction in the gaps and increasing the Fermi potential of the guide system, together with an increase in the proton beam current and optimization of the proton beam tune, should result in a substantial improvement in the UCN  $\beta$  decay rate and the statistical uncertainty. Significant improvements in the limits placed on the fraction of depolarized UCN should follow from higher statistics for depolarization studies and reduced backgrounds in our  $^3\text{He}$  detectors by operating them at higher gain and with better shielding. The systematic errors in electron detection due to backscattering and angle ef-

fects are dominated by scattering in the decay trap and MWPC foils, and can be reduced by at least a factor of 2 (based on Monte Carlo studies) by using  $0.7 \mu\text{m}$  decay trap foils and  $6 \mu\text{m}$  MWPC foils. Uncertainties due to nonlinearity effects can be reduced by an order of magnitude by using a greater selection of calibration sources ( $^{109}\text{Cd}$ ,  $^{134}\text{Ce}$ ,  $^{114\text{m}}\text{In}$ ,  $^{113}\text{Sn}$ ,  $^{85}\text{Sr}$ , and  $^{207}\text{Bi}$ ) and more extensive studies of the detector response. The improvements discussed above should permit a substantial improvement in the precision of our result, making our ultracold neutron experiment competitive with the existing cold neutron beam experiments and providing useful data on the weak interaction of the nucleon.

This work was supported in part by the Department of Energy, National Science Foundation, and Los Alamos National Laboratory LDRD. We acknowledge helpful discussions with A. P. Serebrov.

- [1] A. Czarnecki, W. J. Marciano, and A. Sirlin, Phys. Rev. D **70**, 093006 (2004).
- [2] K. Hagiwara, S. Matsumoto, and Y. Yamada, Phys. Rev. Lett. **75**, 3605 (1995); A. Kurylov and M. J. Ramsey-Musolf, *ibid.* **88**, 071804 (2002).
- [3] N. Severijns, M. Beck, and O. Naviliat-Cuncic, Rev. Mod. Phys. **78**, 991 (2006).
- [4] J. S. Nico and W. M. Snow, Annu. Rev. Nucl. Part. Sci. **55**, 27 (2005).
- [5] H. Abele *et al.*, Phys. Rev. Lett. **88**, 211801 (2002).
- [6] P. Liaud *et al.*, Nucl. Phys. A **612**, 53 (1997).
- [7] Yu. A. Mostovoi *et al.*, Phys. At. Nucl. **64**, 1955 (2001).
- [8] P. Bopp *et al.*, Phys. Rev. Lett. **56**, 919 (1986).
- [9] V. E. Krohn and G. R. Ringo, Phys. Lett. B **55**, 175 (1975).
- [10] J. D. Jackson, S. B. Trieman, and H. W. Wyld, Jr., Phys. Rev. **106**, 517 (1957); B. R. Holstein, Rev. Mod. Phys. **46**, 789 (1974); S. Gardner and C. Zhang, Phys. Rev. Lett. **86**, 5666 (2001).
- [11] W. J. Marciano and A. Sirlin, Phys. Rev. Lett. **96**, 032002 (2006).
- [12] R. Golub, D. J. Richardson, and S. K. Lamoreaux, *Ultra-Cold Neutrons* (Adam Hilger, Bristol, 1991).
- [13] A. Saunders *et al.*, Phys. Lett. B **593**, 55 (2004).
- [14] In the current geometry, UCN are confined to the decay trap, located in a uniform field region, ensuring magnetic mirroring corrections in nonuniform fields to be below the 0.1% level.
- [15] B. Plaster *et al.*, Nucl. Instrum. Methods Phys. Res., Sect. A **595**, 587 (2008).
- [16] T. M. Ito *et al.*, Nucl. Instrum. Methods Phys. Res., Sect. A **571**, 676 (2007).
- [17] S. Agostinelli *et al.*, Nucl. Instrum. Methods Phys. Res., Sect. A **506**, 250 (2003); <http://geant4.cern.ch/>.
- [18] F. Salvat, J. M. Fernández-Varea, and J. Sempau, *PENELOPE-A Code System for Monte Carlo Simulation of Electron and Photon Transport* (Universitat de Barcelona, Spain, 2003).
- [19] J. W. Martin *et al.*, Phys. Rev. C **73**, 015501 (2006).
- [20] F. Gluck and K. Toth, Phys. Rev. D **46**, 2090 (1992).